Biomech Model Mechanobiol (2009) 8:67–76
DOI 10.1007/s10237-008-0121-6

ORIGINAL PAPER

Characterization of human passive muscles for impact loads using genetic algorithm and inverse finite element methods

A. Chawla · S. Mukherjee · B. Karthikeyan

Received: 30 May 2006 / Accepted: 31 January 2008 / Published online: 22 February 2008

Abstract The objective of this study is to identify the dynamic material properties of human passive muscle tissues for the strain rates relevant to automobile crashes. A novel methodology involving genetic algorithm (GA) and finite element method is implemented to estimate the material parameters by inverse mapping the impact test data. Isolated unconfined impact tests for average strain rates ranging from $136\,s^{-1}$ to $262\,s^{-1}$ are performed on muscle tissues. Passive muscle tissues are modelled as isotropic, linear and viscoelastic material using three-element Zener model available in PAMCRASH^{TM} explicit finite element software. In the GA based identification process, fitness values are calculated by comparing the estimated finite element forces with the measured experimental forces. Linear viscoelastic material parameters (bulk modulus, short term shear modulus and long term shear modulus) are thus identified at strain rates $136\,s^{-1}$, $183\,s^{-1}$ and $262\,s^{-1}$ for modelling muscles. Extracted optimal parameters from this study are comparable with reported parameters in literature. Bulk modulus and short term shear modulus are found to be more influential in predicting the stress-strain response than long term shear modulus for the considered strain rates. Variations within the set of parameters identified at different strain rates indicate the need for new or improved material model, which is capable of capturing the strain rate dependency of passive muscle response with single set of material parameters for wide range of strain rates.

Keywords Passive muscle · Viscoelastic material properties · Genetic algorithm · Inverse characterization method · Impact load

A. Chawla (✉) · S. Mukherjee · B. Karthikeyan
Indian Institute of Technology Delhi, Delhi, India
e-mail: achawla@mech.iitd.ernet.in
URL: http://paniit.iitd.ac.in/~achawla/

1 Introduction

Human body finite element models are being developed to simulate automobile crashes in order to understand the injury patterns and injury mechanism pertaining to pedestrians and occupants (Maeno and Hasewaga 2001). The closeness of capturing the injury mechanisms and patterns are directly influenced by the accuracy of tissue properties available. Hence development of the human body finite element models are limited by the knowledge of material behaviour of hard and soft tissues at strain rates experienced during automobile crashes.

Soft tissues exhibit large deformation, viscoelasticity, strain rate dependency and many more unresolved issues due to its complex nature. To characterize the tissue behaviour, several testing methods or procedures have been established by developing problem-specific material models and parameters, which work only for specific domains typically involving lower strain rates. These procedures need further development before these properties can be used for a wide range of conditions as those in vehicle impacts at different speeds.

McElhaney (1966) conducted in vitro test on bovine muscle for dynamic loadings for strain rates up to 1000/s. Viscoelastic response of live skeletal muscles have been investigated by Best et al. (1994) and Myers et al. (1998) for tensile loading at lower strain rates (less than 100/s). Bosboom et al. (2001) measured the mechanical properties of rat skeletal muscle under in vivo compression applied transverse to the muscle fiber direction. Dhaliwal et al. (2002) conducted low energy impact tests on volunteers and human cadavers. Sligtenhorst et al. (2006) determined the bovine muscle properties for strain rates ranging from 1,000 to $2{,}500\,s^{-1}$.

However, properties of different human muscles under transverse impact loading are not yet fully known. The

available properties thus cannot be used to represent the human muscle in pedestrian impacts. Existing Finite Element Human body models use a three-element linear viscoelastic material model to model the muscle tissues (Bandak et al. 2001; Lizee et al. 1998; Chawla et al. 2004). The suitability of other material models like Prony series based models and QLV theory model to impact loads is not yet established in the literature. In the current study we, therefore, use the three element linear visco-elastic model for representing the soft tissue and try and estimate the parameters for the same.

We use an inverse characterization based method to estimate the parameters of the linear visco-elastic model at different strain rates. Controlled tests have been conducted and an iterative procedure is then used for parameter estimation by comparing the experimental and theoretical response for different material inputs (Karthikeyan et al. 2006). Such inverse characterization methods using quasi-static compression experiments (Miller and Chinzei 1997; Miller-Young et al. 2002), ramp tests (Bosboom et al. 2001), aspiration experiments (Kauer et al. 2002) and indentation tests (Durand-Reville et al. 2004; Delalleau et al. 2006; Erdemir et al. 2006) have been reported to characterize the soft tissues at lower strain rates, less than 100/s using optimization techniques. Most of these studies use the conventional search techniques such as direct search methods or gradient-based optimization algorithms (Erdemir et al. 2006; Kauer et al. 2002; Moulton et al. 1995) and couple with finite element methods to obtain the optimal properties for modelling the soft tissue behaviour. Direct search methods use objective function(s) and constraint(s) for searching the optimal parameter(s), and consume more time to converge. Gradient-based methods involve the derivatives along with the objective function(s) and or constrain(s) for faster convergence but they are not efficient in discontinuous and non-differentiable problems (Deb 1999). Both these methods are influenced by the initial solution chosen and can lead to local optima and are not efficient in solving multi-optima problems. Recent trends in the literature have shown that the application of evolutionary algorithms like Genetic algorithms (GA) can overcome the above mentioned problems in inverse characterization studies (Muc and Gurba 2001; Liu et al. 2002a,b; Rahul et al. 2006; Chwastek and Szczglowski 2006) for extracting the optimal parameters.

Studies for identifying the impact properties of passive muscle using GA have not been reported so far to the authors' knowledge. Hence the applicability of this global optimization method, for characterizing the passive muscle tissue, is explored in this study.

In this paper, a feasible Genetic algorithm (GA) based procedure to map the experimental force data to a form that is directly useful for finite element simulations have been formulated. Passive muscle tissues are modelled using linear viscoelastic material model and the values of bulk modulus, short term shear modulus and long term shear modulus are iterated. Optimal material parameters extracted for the strain rates at 136, 183 and 262 s^{-1} are presented in this paper.

2 Genetic algorithms

Genetic algorithms (GAs) are global search and optimization methods based on Darwin's natural evolution theory with underlying principle, "survival of fittest".

2.1 Summary of the GA process

Genetic algorithms evaluate the fitness of individual designs in a population. The size of the population is the number of (feasible) alternatives (called chromosomes, and represented as strings) involved in a particular generation. The population for the first generation is created randomly within the predefined variable range. Based on the fitness values of the strings, GAs then use three basic operators namely the selection, crossover and mutation operators to generate new populations from generation to generation. In the process they produce populations with better chromosomes. The algorithm stops when a predefined convergence criterion is reached (no significant change in the best fitness value in successive iterations). In the absence of convergence the process can be terminated after a predefined number of generations and the best fitness value reported. The present study is conducted using the termination criterion of 50 generations. More details on GAs can be found in Goldberg (1989) and Deb (1995, 2001).

2.1.1 The selection operator

Selection operator reproduces the stronger (better) strings in a population and eliminates the weaker ones. Eliminated strings are replaced by additional copies of the better string thereby improving the average quality of the population. The strings generated after reproduction are called parent solutions and are sent to a mating pool for cross over and mutation. The selection operator only creates copies of the existing good strings and does not create new strings. New chromosomes (called children solutions) are generated using crossover and mutation operators.

2.1.2 The crossover operator

In crossover operations, two parent strings are first selected based on a crossover probability. A part of the first parent string is then interchanged with the other parent's string to produce a child solution. A number of types of crossover operators, based on how the crossover of the bits is done, are used in practice. For instance, in the fixed point crossover

a position is chosen in the binary string representing the parents and all bits to one side of the position are interchanged between the two parents to produce the children.

Real-coded GAs with the simulated binary crossover (SBX) operator are known to perform well specially in problems having multiple optima. It also maintains the variable bounds in the children. Details of real coded GAs and the SBX operator are given in Deb and Agrawal (1995). In this study we use real coded GAs with the SBX operator.

2.1.3 Mutation

The mutation operator selects a parent solution based on a mutation probability and changes one bit in the sting from 1 to 0 or from 0 to 1 to produce a new child solution.

3 Methods

A schematic diagram to identify the material properties of passive muscle tissue using genetic algorithm approach and finite element methods is shown in Fig. 1. First, the experimental force – time response from the isolated impact tests are obtained. Finite element model representing the experimental condition is then developed. Soft tissue material properties form the design parameters in the optimization stage. In each run of the finite element model these parameters are incorporated as per the estimates from the genetic algorithm for the respective population. The corresponding finite element force response is then calculated. Finite element force – time response is compared with the reference experimental force – time response to evaluate the objective function for GA. Material parameters undergo fitness evaluation in the matting pool through selection, cross over and mutation process for generating new material estimate for the next generation. The process is continued for a predefined number of generations, and convergence is observed.

3.1 GA implementation

The GA code utilized in the present study was adopted from Kanpur Genetic Algorithms Laboratory (KanGAL), Indian Institute of Technology Kanpur. This code was modified for parameter identification of passive muscle tissue by generating responses of members of a population through finite element analysis in order to match the response of impact tests on isolated tissue specimen. Real coded GA with rigid bound condition on the variable selection is used with tournament selection. We use simulated binary crossover with a probability of 0.9 and distribution index 10 and polynomial mutation with a probability of 0.1 and distribution index 20. These parameters are shown in Table 1. This table also indicates the selected variables for iteration, their rigid bounds

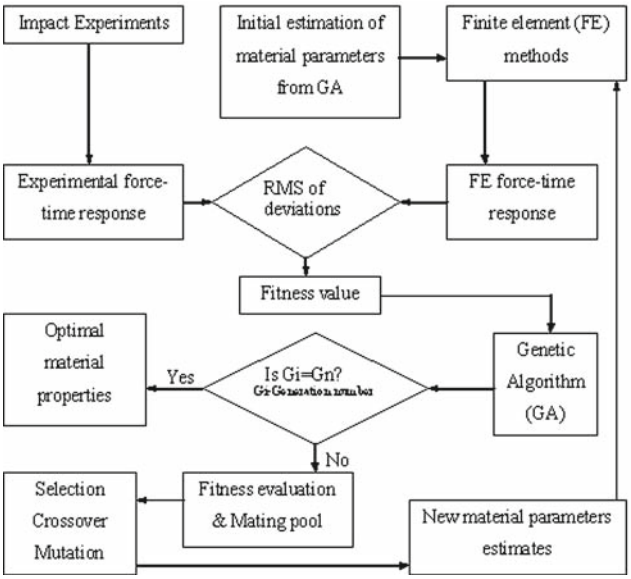

Fig. 1 Schematic layout of GA based material parameter identification process

and the random seed probability used for initial population selection. The initial population is generated as a random distribution within the defined variable bounds. The GA process is considered to converge when the best fitness in successive iterations no longer produce better results.

3.2 Fitness calculation

The objective function of the problem is to minimize the root mean square (RMS) differences between experimental and finite element force responses as indicated in Eq. (1) and (2).

$$\text{Fitness}, \quad f(X) = \sqrt{\frac{\Sigma_i^n \left(F_i^{\exp} - F_i^{\text{fem}}\right)^2}{n}} \tag{1}$$

where $F_i^{\exp}$ is the experimental force response, F_i^{fem} is the finite element force response, and n is the number of data points.

The problem can be stated as follows:

$$\text{Minimize } f(X) \tag{2}$$

for

$$K_{\min} < K < K_{\max}$$
$$G_{0\min} < G_0 < G_{0\max}$$
$$G_{1\min} < G_1 < G_{1\max}$$

Subjected to constraints

$$K - G_0 > 0, \tag{3}$$
$$G_0 - G_1 > 0 \tag{4}$$

Table 1 GA input parameters

Description of function	Value (units)
Number of generations	50
Population size	80
Number of real coded variables	3
Variables iterated	K, G_0 and G_1
Lower and upper bound of K	$(K)_{\min} = 1E+03$ (Pa), $(K)_{\max} = 1E+07$ (Pa)
Lower and upper bound of G_0	$(G_0)_{\min} = 1E+02$ (Pa), $(G_0)_{\max} = 1E+06$ (Pa)
Lower and upper bound of G_1	$(G_1)_{\min} = 1E+02$ (Pa), $(G_1)_{\max} = 1E+06$ (Pa),
Are the variables real bounds rigid	Yes
Cross over probability	0.8
Mutation probability for real variables	$1/n$ (n is the population size)
Distribution index for SBX	10
Distribution index for mutation	20
Give random seed (0 to 1)	0.875

where K is the bulk modulus, G_0 is the short term shear modulus, and G_1 is the Long term shear modulus.

Bulk modulus, short term shear modulus and long term shear modulus are selected as material variables and are iterated for minimizing the fitness. Two constraints (Eq. (3) and (4)), state that the bulk modulus should be greater than short term shear modulus and long term shear modulus should be the lowest among all three are applied (Lizee et al. 1998).

3.3 Experimental data

Experimental force response (Karthikeyan et al. 2006) obtained from nineteen impact tests on unconfined isolated human muscles for strain rate ranging from 136 to 262 s^{-1} is used as the target response. All these tests have been conducted for a maximum compression of approximately 50% strain. The experimental data has been presented in Karthikeyan et al. (2006) and is briefly described here for completeness. Data are grouped for three average strain rates 136/s ($n = 7$), 183/s ($n = 5$) and 262/s ($n = 7$) and used for parameter estimation.

3.3.1 Specimen preparation

Surgical scrap consisting of healthy muscles from three living human subjects and obtained from All India of Medical Sciences (AIIMS).

The tissues are identified as Human1 (H1), Human2 (H2) and Human3 (H3). The regional location of the tissues and the number of samples tested are indicated in Table 2. Tissues H1 and H2 are from the lower extremity region (thigh) while tissue H3 is from the upper extremity region (shoulder). All the specimens collected after the surgery were wrapped in polythene sheet and frozen at −20°C for 2 weeks (Van Ee et al. 1998, 2000). Three hours before testing, specimens are thawed at 20°C and the fascia layer is removed from the tissue. Measures are taken to prevent the dehydration of the tissue during testing. No other preconditioning has been done before conducting the tests.

Table 2 Subject Identification (reproduced from Karthikeyan et al. 2006)

Subject Identification	Muscle region in the human body	Number of specimens tested
H1	Lower extremity	3
H2	Lower extremity	8
H3	Upper extremity	21

Cubic specimens with a square cross section of 14 × 14 mm are prepared using a scalpel. The dimensions have a deviation of about 0.25 – 0.5 mm. The sample height is measured in the direction perpendicular to fiber orientation in the anterior–posterior direction and is listed in Table 3. A total of 32 specimens were prepared.

3.3.2 Experimental set-up

A custom made spring loaded machine is used to impact the specimen. The spring is wound to the desired level using a motorized mechanism and released to launch a 1 kg impactor. A velocity up to 8 m/s can be achieved. A strain gage based force transducer (S-Type) capable of measuring both static and dynamic forces up to 1,000 N is mounted below the bottom platen. A high-speed motion camera (REDLAKE, San Diego, CA, USA) is used to record the impact. The video is subsequently analyzed to find out the displacement of the

Table 3 Successful tests and individual strain rate along with the measured initial velocity (reproduced from Karthikeyan et al. 2006)

Subject ID–Test ID	Specimen height (mm)	Initial velocity (m/s)	Strain rate (s^{-1})	Strain rate group (Mean ± SD, n)
H2–T07	9.5	1.23	129	Lower strain rate (136 ± 19.94, $n = 7$)
H3–T01	8.5	1.13	133	
H3–T03	11.0	1.18	107	
H3–T04	9.0	1.20	134	
H3–T10	9.5	1.21	127	
H3–T11	7.5	1.22	163	
H3–T12	7.5	1.22	162	
H3–T05	10.5	1.80	172	Medium strain rate (183 ± 6.80, $n = 5$)
H3–T06	9.0	1.72	191	
H3–T07	9.0	1.66	184	
H3–T15	10.0	1.83	183	
H3–T17	10.5	1.92	183	
H1–T03	8.5	2.30	271	Higher strain rate (262 ± 31.63, $n = 7$)
H2–T05	8.0	2.27	284	
H2–T06	7.5	2.18	291	
H2–T08	10.0	2.07	207	
H3–T08	8.5	2.30	271	
H3–T09	8.5	2.40	282	
H3–T19	10.5	2.40	229	

tissue and the initial velocity of the impactor. A strain gauged cantilever beam is kept at the same level as the tissue top surface. The beam has a trigger switch, which is set to trigger the data acquisition as well as the video recording. It also synchronizes the force and displacement data and helps to identify the start of the event. Data is acquired using an e-DAQ system (SoMat Corporation, Urbana, IL, USA). Specimen compression level is controlled using a rigid mechanical stopper, which constrains the motion of the top platen after the tissue gets compressed to the required strain (which is 50% in all the tests reported in this paper).

In order to minimize friction between with the top and bottom surfaces Poly Ttetra Flouro Ethylene (PTFE) sheets are used as interface between the bottom platen and specimen to reduce friction and insulation tapes were wrapped at the contacting surface of the top platen. The tests are done using unconfined specimen so as to minimize the viscous and frictional effects. Repeatability of the impact test set-up has been established and presented in Karthikeyan et al. (2006).

3.3.3 Experimental protocol

Tests were conducted for three different initial impact velocities (1.20 ± 0.03 m/s, 1.79 ± 0.1 m/s and 2.27 ± 0.12 m/s) resulting in the mean (standard deviation) strain rates of 136 s^{-1} (19.9 s^{-1}), 183 s^{-1} (6.8 s^{-1}) and 262 s^{-1} (31.3 s^{-1}). List of tests and the strain rates are given in the Table 3. Out of the 32 tests conducted, 7 were performed successfully at an average strain rate of 136 s^{-1}, 5 tests at 183 s^{-1} and 7 at 262 s^{-1}, amounting to a total of 19 successful tests. Force data is acquired at 10000 samples per second. Video is recorded at 5000 frames per second with a resolution of 384 × 256 pixels for 0.05 seconds before trigger and 0.49 seconds after trigger.

3.3.4 Data analysis

Acquired force data is post processed with N-soft^{TM} (NCode, Sheffield, UK) data analysis package. The displacement and velocity data is obtained by analyzing the recorded video using Image Express^{TM} software. Engineering stresses and engineering strains are calculated from this force and displacement data. Initial velocity of the impactor is calculated by taking the average of 10 velocity data points obtained from the video analysis. These represent duration of about 2 milliseconds before the start of impact. Strain rate is calculated as the ratio of initial velocity and initial specimen height. The strain rate was observed to be constant throughout each test with a maximum variation of 10% from the mean. During post processing of the force data, the sample rate is reduced from 10,000 samples per second to 5000 samples per second so as to synchronize it with the deflection data. Out of the 32 tests conducted, data of 13 tests have not been used because of problems with the experimental data.

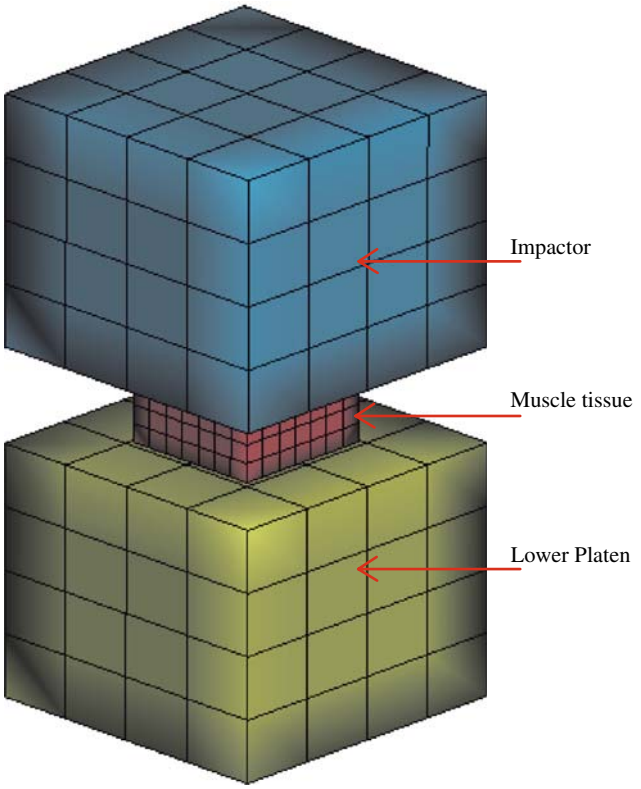

Fig. 2 Finite element model of soft tissue, top and bottom platen

3.4 Finite element modelling

Since the finite element (FE) technique can predict the response of a material to a given loading well, we use the FE method for this purpose. The choice was also governed by the fact that the results of the study will be used in developing FE models.

3.4.1 Model description

Finite elements (FE) mesh of the top platen, bottom platen and muscle tissue is generated in I-deas^{TM} (UGS-PLM solutions, USA) using eight-node solid elements. Finite element modelling, simulations and post-processing are performed using PAM-System of software (ESI group, France). The FE model indicated in Fig. 2 consists of 373 elements and 634 nodes. Element quality has been ensured by keeping the aspect ratio less than 3 and the wrap angle less than 10°.

3.4.2 Selecting the finite element mesh

Convergence of the FE model has been established to decide the mesh size and number of elements (Miller et al. 2000). The FE model with different mesh sizes is simulated and the force response is observed. When the variation in the response is less than 5% between two successive mesh sizes, then the larger mesh is selected for further analysis.

We use the PAMCRASH^{TM} explicit FE software as explicit methods have better convergence and are less expensive than the implicit methods in large deformation problems. In order to ensure convergence and stability, PAMCRASH^{TM} uses the following time step criterion (Pam System International 2000):

$$\Delta t_{\text{elemental}} = \frac{L_C}{C_0} \tag{5}$$

since $C_0 = \sqrt{\frac{E}{\rho}}$, the above equation can be written as

$$\Delta t_{\text{elemental}} = L_C \sqrt{\frac{\rho}{E}} \tag{6}$$

where L_C is the characteristic length, C_0 material speed, E the elastic modulus, ρ the mass density of the element.

Typical minimum time step in the present study is observed to be above 0.8 μs.

3.4.3 Material description

Soft tissue is represented as linear viscoelastic material model and is described in Eq. 7 (Pam System International 2000):

$$G(t) = G_1 + (G_0 - G_1)\mathrm{e}^{-\beta t} \tag{7}$$

where $G(t)$ is the shear relaxation behaviour, G_1 is the long term shear modulus, G_0 is the short term shear modulus and β is the decay constant.

Top and bottom platen are modelled using elastic–plastic material model with steel properties. The material properties of bottom and top platen are indicated in Table 4. This table also indicates the initial material property chosen for soft tissue to calculate the fitness value at the start of GA execution. The initial estimates of bulk modulus, short term shear modulus and long term shear modulus of muscle specimen will be replaced with new estimates during parameter identification process.

3.4.4 Contact definition and boundary conditions

Two individual contact definitions are defined between the muscle tissue and the top platen, muscle tissue and bottom platen. The bottom platen is constrained for zero displacement in all directions. A free translation of top platen is allowed in the axial (vertical Z) direction while the lateral translations (horizontal X and Y) and all rotations are constrained for zero displacements. Frictional coefficient of 0.3 (Wu et al. 2004) is applied. Specimen is defined with additional self-contact definition incorporating solid anti-collapse to prevent interlocking during large deformations. Displacement of the tissue is measured at the center node

Table 4 Initial material properties of soft tissue and top and bottom platen

Soft tissue represented as linear viscoelastic material				
Bulk modulus, K (Pa)	Short-term shear modulus, G_0 (Pa)	Long-term shear modulus, G_1 (Pa)	Decay constant, β (s^{-1})	Density, ρ (kg/m^3)
1.00E+06	1.00E+05	1.00E+04	100	1,000
Top and bottom platen represented as elastic–plastic material				
Bulk modulus (Pa)	Yield stress (Pa)	Tangent modulus (Pa)	Shear modulus (Pa)	Density (kg/m^3)
1.75E+11	2.90E+08	8.00E+07	8.08E+10	7,820

on the top surface of the tissue mesh and the axial force is observed from the rigid wall contact force.

3.4.5 Automation of FE solutions

A C++ program has been written to link PAMCRASH^{TM} with the main GA code. This has been done using a protocol in which whenever the PAMCRASH^{TM} file is to be executed, the following steps are carried out.

1. PAMCRASH ^{TM} input file is generated
2. PAMCRASH ^{TM} solver is run
3. the output file generated is interpreted so as to present the desired variables (the force deflection histories) in an ASCII format readable in C++

These steps have to be followed for evaluating the objective function for each individual member of the population.

3.4.6 Simulation protocol and data analysis

Parameter identification of passive muscle tissue from isolated impact tests data is performed for each set of tests with a common target strain rate.

We use nineteen experimental force responses as reference data for calculating the fitness values. This data are grouped into three average strain rates of 136, 183 and 262 s^{-1} for analysis.

Though the prediction of different set of material properties at different strain rates may indicate the strain rate dependency of the material model, an additional analysis subjecting the relative initial velocities of other strain rates with the same material property has been performed as a cross checking process. This analysis is preformed by applying initial velocity corresponding to 183 and 262 s^{-1} for the model having optimal material properties of 136 s^{-1}. Similarly the optimal material properties obtained at 183 and 262 s^{-1} are tested for other average strain rates 136, 262 s^{-1} and 136, 183 s^{-1} respectively.

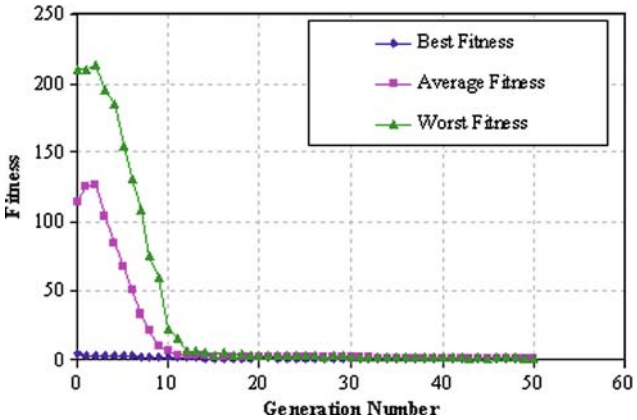

Fig. 3 Convergence plot for average strain rate 136 s^{-1}

4 Results and discussion

Parameter identification of linear viscoelastic material properties of passive muscle has been performed using inverse characterization based on GAs and experiments conducted on a common target strain rate. The full GA optimization process takes about 9 h 41 min (34,860 s) on an Intel P4 Dual core 3 GHz processor with 1 GB RAM and the Windows XP operating system. We now discuss the results obtained.

4.1 GA results

The best fitness, average fitness and worst fitness calculated at each generation for the average strain rate 136 s^{-1} is shown typically in Fig. 3. This figure shows the convergence of optimization solution. Similar behaviour is also observed at other strain rates. As the function is minimized for obtaining the optimal fit, the decreasing trend in the fitness values is seen at all strain rates. For the study conducted at strain rate 136 s^{-1}, the optimal fitness is observed at 45th generation. Similarly other optimums are reached at 34 and 15 generation for strain rates 183 and 262 s^{-1} respectively. Table 5 lists the material properties obtained. An additional data from Lizee et al. (1998) is also presented for relative comparison though the data does not report the strain rate at which the properties are extracted.

Table 5 Comparison of material properties of soft tissues at different strain rates

Reference	Average strain rate (s^{-1})	Bulk modulus, K (Pa)	Short-term shear modulus, G_0 (Pa)	Long-term shear modulus, G_1 (Pa)
Lizee et al. (1998)	–	250,000	115,000	86,000
Present study	136	72,680	11,700	239.1
Present study	183	276,300	25,520	617.6
Present study	262	298,600	39,950	2,949

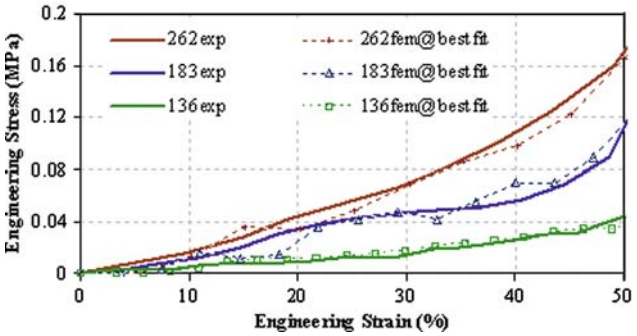

Fig. 4 Stress–strain curves of experimental response and optimal FE response for the material properties extracted for common target strain rates

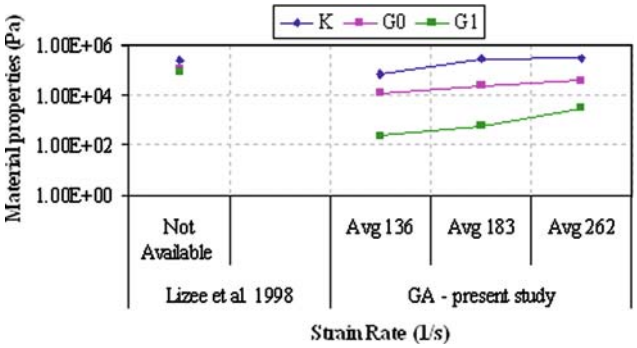

Fig. 5 Comparative studies of material properties at various strain rates

The stress–strain response of experimental and GA based FE approach for the strain rates 136, 183 and 262 s^{-1} are shown in Fig. 4. The finite element stress strain response is obtained by substituting the best-fit material properties in the FE model. A good match is observed between the experimental and the finite element stress strain response at all strain rates.

Figure 5 indicates the variation of material properties identified at different strain rates. Though the magnitude of all the properties considered increases with increase in strain rate, the long term shear modulus has been found to be least influential as it governs the response only at slow strain rates. The instantaneous response of the linear viscoelastic model is governed by short term shear modulus. As all the FE models have been subjected to higher strain rates in the study, the influence of short term shear modulus as observed is expected.

Table 6 Maximum stress corresponding different material inputs and strain rates

Strain rate (s^{-1})	Corresponding strain rate of material input (s^{-1})	Maximum stress at 50% strain (MPa)
136	Experiment	0.044
136	136	0.037
183	136	0.040
262	136	0.046
183	Experiment	0.114
136	183	0.079
183	183	0.115
262	183	0.088
262	Experiment	0.170
136	262	0.140
183	262	0.142
262	262	0.165

4.2 Strain rate independency of material model

Linear viscoelastic material model is found to be incapable of capturing the stain rate dependency of passive muscle with single set of material parameters for the tested strain rates 136, 183 and 262 s^{-1}.

With a single short term shear modulus and long term shear modulus, the model does not reproduce the stress-strain response obtained in experiments. To model the strain rate dependency of the tissue by subjecting to different strain rates, the linear viscoelastic model requires multiple set of material properties to reproduce the experimental response of the muscle. This phenomenon is tested by subjecting the FE model with different velocities to a single set of material properties. The stress at 50% strain is indicated in Table 6 for the material inputs extracted from the corresponding strain rates and material inputs taken from the different strain rates.

Little variations are found in the stress values for the studies conducted at different strain rates but with identical material properties. It can be observed when the FE model is subjected to higher strain rate (262 s^{-1}, properties are

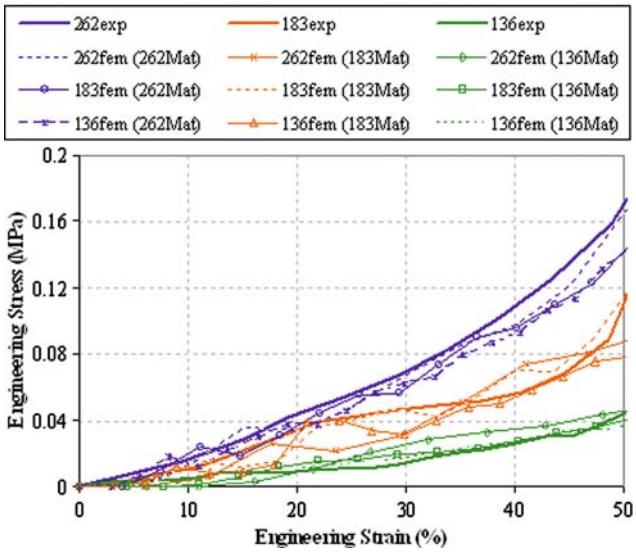

Fig. 6 Comparison of stress-strain response with single set of input set of material properties and multiple sets of material properties for various strain rates

extracted at 136 s^{-1}) without change in material property the FE stresses (0.046 MPa) are not comparable with the experimental values (0.165 MPa) as the model does not reflect the strain rate dependency. On the other way, when the FE model is subjected to the material inputs extracted at respective strain rates, the finite element stresses are comparable with the experimental conditions. The properties extracted from the respective strain rates are called as single material properties and the properties extracted from the other strain rates are indicated as multiple material properties throughout this text. The comparison of experimental and finite element response for the material property extracted from the respective strain rates and material properties extracted from the other strain rates is shown in Fig. 6. The stress strain response indicates that the linear viscoelastic material model is capable of capturing the strain rate dependency with material properties extracted at the respective strain rates. But this mechanism cannot be used for conducting the full body simulations where different impact velocities are experienced. Hence a new or improved material model, which is capable of capturing the strain rate dependency of passive muscle response with single set of material parameters for wide range of strain rates, is expected.

5 Conclusion

A procedure to map the experimental data from tests over a range of strain rates and strain magnitude to a form that can be useful for finite element simulations using genetic algorithm has been established. Viscoelastic material properties obtained for strain rates at 136, 183 and 262 s^{-1} are presented and compared with those available in literature. Finite element stress–strain responses are found to have a better match with the experiment response when properties extracted at that respective strain rate are used in the FE model. This should not be the case for a material, which behaves truly like a viscoelastic material. Thus, we conclude that the linear viscoelastic model, which is widely used to characterize the muscle response in crash studies, is not capable of predicting the strain rate dependency. This indicates the need for new or improved material model.

6 Further improvements and limitations

With the advent of advanced computing facilities the time consumption of GA is not a major concern in the present scenario. Still, the application of this method for characterizing a larger number of variables may require inclusion of parallel processing techniques and improved GA operators as in adaptive GA. More tests are needed for to better characterize the tissues of the different parts of the body and also to study variations in properties with respect to parameters like age and gender. The study has currently been performed for strain rates between 136 and 262 s^{-1}, but can easily be (and is being) extended to higher strain rates. Once the variations in these properties at higher rates is known, a single material law can be defined which will incorporate the strain rate effects.

Acknowledgments The authors would like to acknowledge the Department of Science and Technology of India and the support from the Volvo Research Foundation for funding the study. The last author also wishes to thank Sona Koyo Steering Systems Limited for their support. The authors would like to acknowledge Mr. Balamurugan Ramasamy for his help during code development. The authors are also grateful to KANGAL laboratory for providing the GA code in the public domain.

References

Bandak FA, Tannous RE, Toridis T (2001) On the development of an osseo-ligamentous finite element model of the human ankle joint. Int J Solids Struct 38:1681–1697

Best TM, McElhaney J, William EG, Myres BS (1994) Characterization of the passive response of live skeletal muscle using the quasi-linear theory of viscoelasticity. J Biomech 27:413–419

Bosboom EMH, Hesselink MKC, Oomens CWJ, Bouten CVC, Drost MR, Baaijens FPT (2001) Passive transverse mechanical properties of skeletal muscle under in vivo compression. J Biomech 34:1365–1368

Chawla A, Mukherjee S, Mohan D, Parihar A (2004) Validation of lower extremity in THUMS. In: International IRCOBI conference on the biomechanics of impact, September 22–24, Graz, Austria

Chwastek K, Szczglowski J (2006) Identification of hysteresis model parameters with genetic algorithms. Math Comput Simulat 71:206–211

Deb K (1995) Optimization for engineering design: Algorithms and examples. Prentice-Hall, Delhi

Deb K (1999) An introduction to genetic algorithms. Sadhana 24:205–230

Deb K (2001) Multi-objective optimization using evolutionary algorithms. Wiley, Chichester

Deb K, Agrawal RB (1995) Simulated binary crossover for continuous search space. Complex Syst 9:115–148

Delalleau A, Josse G, Lagarde J, Zahouani H, Bergheau JM (2006) Characterization of the mechanical properties of skin by inverse analysis combined with the indentation test. J Biomech 39:1603–1610

Dhaliwal TS, Beillas P, Chou CC, Prasad P, Yang KH, King AI (2002) Structural response of lower leg muscles in compression: a low impact energy study employing volunteers, cadavers and the Hybrid III. Stapp Car Crash J 46:229–243

Durand-Reville M, Tiller Y, Paccini A, Lefloch A, Delotte J, Bongain A, Chenot JL (2004) Immediate post-operative procedure for identification of the rheological parameters of biological soft tissue. International Congress Series 1268:407–412

Erdemir A, Viveiros ML, Ulbrecht JS, Cavanagh PR (2006) An inverse finite-element model of heel-pad indentation. J Biomech 39:1279–1286

Goldberg DE (1989) Genetic algorithms in search, optimization, and machine learning. Addison-Wesley, New York

Karthikeyan B, Mukherjee S, Chawla A (2006) Soft tissue characterization for compressive loading using experiments and finite element methods.. SAE 2006 Trans J Passenger Cars: Mech Syste 115:173–182

Kauer M, Vuskovic V, Dual J, Szekely G, Bajka M (2002) Inverse finite element characterization of soft tissues. Med Image Anal 6:275–287

Liu GR, Han X, Lam KY (2002) A combined genetic algorithm and nonlinear least squares method for material characterization using elastic waves. Comput Methods Appl Mech Eng 191:1909–1921

Liu GR, Ma WB, Han X (2002) An inverse procedure for determination of material constants of composite laminates using elastic waves. Comput Methods Appl Mech Eng 191:3543–3554

Lizee E, Robin S, Song E, Bertholan N, Lecoz JY, Besnault B, Lavaste F (1998) Development of 3D finite element model of the Human Body. SAE 1998 Trans J Passenger Cars 107:2760–2782

Maeno T, Hasewaga J (2001) Development of a finite element model of the total human model for safety (THUMS) and application to car-pedestrian impacts. In: The 17th international technical conference on the enhanced safety of vehicles, 4–7 June, Amsterdam, The Netherlands

McElhaney J (1966) Dynamic response of bone and muscle tissue. J Appl Physiol 21:1231–1236

Miller K, Chinzei K (1997) Constitutive modelling of brain tissue: experiment and theory. J Biomech 30:1115–1121

Miller K, Chinzei K, Orssengo G, Bednarz P (2000) Mechanical properties of brain tissue in-vivo: experiment and computer simulation. J Biomech 33:1369–1376

Miller-Young JE, Duncan NA, Baroud G (2002) Material properties of the human calcaneal fat pad in compression: experiment and theory. J Biomech 35:1523–1531

Moulton MJ, Creswell LL, Actis RL, Myers KW, Vannier MW, Szabo BA, Pasque MK (1995) An inverse approach to determining myocardial material properties. J Biomech 28:935–948

Muc A, Gurba W (2001) Genetic algorithms and finite element analysis in optimization of composite structures. Compos Struct 54:275–281

Myers BS, Woolley CT, Slotter TL, Garrett WE, Best TM (1998) The influence of strain rate on the passive and stimulated engineering stress-large strain behaviour of the rabbit tibialis anterior muscle. J Biomech Eng 120:126–132

Pam System International (2000) PAM-CRASH PAM-SAFE Version 2000 notes manual. Rungis-Cedex, France

Rahul SG, Chakraborty D, Dutta A (2006) Multi-objective optimization of hybrid laminates subjected to transverse impact. Compos Struct 73:360–369

Sligtenhorst CV, Cronin DS, Brodland GW (2006) High strain rate compressive properties of bovine muscle tissue determined using a split Hopkinson bar apparatus. J Biomech 39:1852–1858

Van Ee CA, Chasse AL, Myers BS (1998) The effect of postmortem time and freezer storage on the mechanical properties of skeletal muscle. SAE 1998 Trans J Passenger Cars 107:2811–2821

Van Ee CA, Chasse AL, Myers BS (2000) Quantifying skeletal muscle properties in cadaveric test specimens: effect of mechanical loading, postmortem time, and freezer storage. J Biomech Eng 122: 9–14

Wu JZ, Dong RG, Schopper AW (2004) Analysis of effects of friction on the deformation behavior of soft tissues in unconfined compression tests. J Biomech 37:147–155